



Porous-reduced graphene oxide for fabricating an amperometric acetylcholinesterase biosensor

Yanping Li, Yunfei Bai, Gaoyi Han*, Miaoyu Li

Institute of Molecular Science, Chemical Biology and Molecular Engineering, Laboratory of Education Ministry, Shanxi University, Taiyuan 030006, PR China

ARTICLE INFO

Article history:

Received 14 February 2013

Received in revised form 16 May 2013

Accepted 17 May 2013

Available online 25 May 2013

Keywords:

Acetylcholinesterase

Organophosphorus pesticides

Graphene

Biosensor

ABSTRACT

This work reports a sensitive amperometric biosensor for organophosphate pesticides (OPs) fabricated through modifying glassy carbon electrode with acetylcholinesterase (AChE) immobilized on porous-reduced graphene oxide (pRGO). The pRGO sheets can not only provide high surface area but also facilitate the diffusion and mass transport of reactants. The as-prepared biosensor shows high affinity to acetylthiocholine (ATCl) with a Michaelis–Menten constant value of 0.73 mM. Furthermore, based on the inhibition of the enzymatic activity (immobilized AChE) caused by the model compound of carbaryl (one kind of pesticides), it is found that the inhibition activity of carbaryl is proportional to its concentration ranging from 0.001 to 0.05 $\mu\text{g mL}^{-1}$. The developed biosensor shows a detection limit of 0.5 ng mL^{-1} for OPs detection and exhibits good performance such as reproducibility and stability, which makes it possible to provide a new and promising tool for the analysis of enzyme inhibitors.

© 2013 Elsevier B.V. All rights reserved.

1. Introduction

Organophosphate compounds, as the most commonly applied pesticides in agriculture, are proved to be the typical insecticide exhibiting fairly high toxicity. With the exploitation of many pesticides, the rapid, reliable, qualitative and quantitative determinations of trace levels of these compounds are significant to health and the environment [1]. A combination of enzymatic reactions with the electrochemical method allows the development of different enzyme-based electrochemical biosensors for environmental analysis [2]. Among these, amperometric acetylcholinesterase (AChE) biosensors have shown satisfactory result for organophosphate pesticides (OPs) determination based on the inhibition of AChE [3,4], which the enzyme activity is employed as an indicator for quantitative measurement of insecticides. When AChE is immobilized on the working electrode surface, its interactions with the acetylthiocholine (ATCl, substrate) produce the electro-active product of thiocholine. The inhibition on the enzyme system can be monitored by measuring the oxidation current of thiocholine [2]. As an alternative strategy, many nanomaterials including gold nanoparticles, carbon nanotubes and so on have been employed to fabricate AChE biosensors with good performance including high sensitivity, rapid response and good stability [5–9].

Graphene, as a new two-dimensional carbon nanomaterial, has attracted increasing attention during recent years by virtue

of its outstanding physical, chemical properties and excellent electrocatalytic ability. According to recent reports [10–14], the special properties of graphene may provide insight into the fabrication of novel biosensors for virtual applications: the high surface area is helpful in increasing the surface loading of the target enzyme molecules, the excellent conductivity and small band gap are favorable for conducting electrons from the biomolecules [15]; and graphene-based chemical sensors reported previously have a much higher sensitivity because of the low electronic noise from thermal effect [16]. Ionic liquid-functionalized graphene [17], CdS-decorated graphene nanocomposite [18], TiO₂-decorated graphene nanohybrid [19], nanohybrid of gold nanoparticles and chemically reduced graphene oxide nanosheets [20] and 3-carboxyphenylboronic acid/reduced graphene oxide/gold nanocomposites [21] have been employed to fabricate AChE biosensors which show good performance including high sensitivity, rapid response and good stability.

Graphene and graphene-based composite materials possessing three-dimensional (3D) porous architectures are preferred for the aforementioned applications owing to their very large surface areas and low mass transport resistance. Recently, porous graphene has stimulated much interest due to its potential applications in gas separation [22], nanoelectronics, hydrogen storage [23] and many other fields [24–26]. Compared with graphene, porous graphene shows improved performance in electronic devices [24], supercapacitors [25] and gas sensors [26]. Porous graphene should also be very useful as a new support because porous supports can not only provide high surface area but also facilitate the diffusion and mass transport of reactants [27–30].

* Corresponding author. Tel.: +86 351 7010699; fax: +86 351 7010699.
E-mail address: han.gaoyi@sxu.edu.cn (G. Han).

To the best of our knowledge, the AChE biosensor based on porous graphene has not been developed. In an effort to develop a highly sensitive biosensing platform for OPs, we have explored the utilization of as-prepared porous reduced graphene oxide (pRGO) as an immobilization matrix. The immobilized AChE exhibits great affinity to its substrate and excellent catalytic effect on the hydrolysis of ATCl. Since AChE is the target of OPs, the proposed enzyme-based biosensors have been developed as a new method for monitoring of trace OPs based on their inhibitions. In order to estimate the properties of the interface, such characterization techniques as cyclic voltammetry (CV) and electrochemical impedance spectroscopy (EIS) are used and a sensitive method for determination of carbaryl is proposed.

2. Experimental

2.1. Materials and reagents

Acetylcholinesterase (AChE, Type C3389, 500 U mg⁻¹ from electric eel), acetylthiocholine chloride (ATCl) and carbaryl were purchased from Sigma–Aldrich (USA) and used without further purification. The pRGO was synthesized in accordance with a published procedure [31]. For comparison, graphene was prepared using the similar procedure without KOH.

Phosphate buffer solution (PBS, 0.1 M, pH 7.4) was prepared by mixing stock standard solutions of NaH₂PO₄ and Na₂HPO₄, and adjusting the pH with 0.1 M NaOH to 7.4. Chitosan (deacetylation, 95%) and other chemicals were of analytical grade and used without further purification, and all solutions were prepared with double distilled water.

2.2. Electrode preparation and modification

Prior to modification, the glassy carbon electrode (GCE) was polished carefully to a mirror-like state with 0.3 and 0.05 μm alumina slurry and sequentially sonicated in 6 M nitric acid, acetone and double distilled water. Then the electrode was rinsed with double distilled water and allowed to dry at room temperature.

Chitosan solution (pH = 5.0, 1.0 mg mL⁻¹) was prepared according to previous report [32]. 2.0 mg pRGO was added to 1.0 mL of 2.0 mg mL⁻¹ chitosan aqueous solution to form homogenous dispersion with sonication. The modified electrode was prepared by a simple casting method as follows: initially, the pretreated GCE was modified by dropping 5.0 μL of the pRGO/chitosan solution and allowed to be dried in ambient air for 4 h to obtain pRGO-CHIT/GCE modified electrode; then the obtained electrode was coated with 5.0 μL AChE solutions (12.5 mU, containing 5 mg mL⁻¹ BSA to maintain the stability of AChE), which were incubated at 25 °C for 30 min; after evaporation of water, the modified electrode was washed with PBS to remove the unbound AChE and the resulted AChE-pRGO-CHIT/GCE was stored at 4 °C. To make a comparison, AChE-CHIT/GCE with the same quantities of AChE was prepared by using the similar procedure.

2.3. Measurement procedure

Inhibition of OPs: the proposed AChE-pRGO-CHIT/GCE was first immersed in 0.1 M PBS containing different concentrations of standard carbaryl solution for 12 min and then transferred to the electrochemical cell of 20.0 mL PBS containing 6.0 mM ATCl to study the electrochemical response by cyclic voltammetry between 0.1 and 1.0 V (vs. SCE). The inhibition of pesticide was calculated as follows: inhibition (%) = $(1 - I_{p,exp}/I_{p,control}) \times 100$, where $I_{p,control}$ is the peak current of ATCl on AChE-pRGO-CHIT/GCE and $I_{p,exp}$ the corresponding peak current of ATCl with pesticide inhibition.

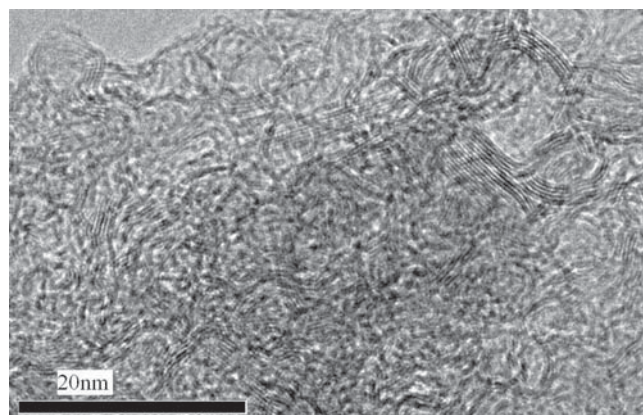


Fig. 1. The HRTEM image of pRGO.

The apparent Michaelis–Menten constant (K_m) of the biosensor can be obtained from the typical current-time plot for the biosensor at 750 mV after the successive addition of ATCl to 0.1 M PBS under stirring. So the K_m value which could give an indication of the enzyme substrate kinetics for the biosensor was determined by analysis of the slope and intercept for the plot of the reciprocals of the steady-state current versus ATCl concentration.

2.4. Instrumentation

The morphologies of the obtained pRGO were observed by using a transmission electron microscope (TEM, JEOL-JEM-1011). Raman spectra were recorded on a JobinYvon Lab RAMHR800 microscopic confocal Raman spectrometer by employing a laser of 514 nm as incident light. The time for each measurement was 30 s and the spectra were recorded by accumulating the measurement for three times. The electrochemical experiments were performed with a CHI660 C electrochemical analyzer (Chen Hua Instruments, Shanghai, China) with a conventional three-electrode system where glassy carbon electrode (GCE, 3 mm in diameter), a saturated calomel electrode (SCE) and platinum wire was used as working electrode, reference electrode and counter electrode, respectively. EIS were performed in a 0.1 M KCl solution containing 5.0 mM Fe(CN)₆^{3-/4-} with a frequency range from 0.1 Hz to 100 kHz at 0.20 V, and the amplitude of the applied sine wave potential in each case was 5 mV.

3. Results and discussion

3.1. Characterization of pRGO

The HRTEM (Fig. 1) showed that the edge had a few irregularly stacked layers and demonstrated that the pRGO sheets consisted of three to seven layers. In contrast to Raman spectra of graphene (Fig. 2a), the upshift of G-band and the downshift of D band for the pRGO (Fig. 2b) could be attributed to the existence of more pores and edges [33,34]. It was also found that Raman spectrum of pRGO exhibited a slightly increased area ratio of D/G relatively to that of graphene (from 1.37 to 1.44). This change might suggest a decrease in the average size of the sp² domains for pRGO [35] and could be well explained by the creation of pores and edges in pRGO.

3.2. Electrochemical impedance spectroscopy

EIS was an effective tool for studying the interface properties of surface-modified electrodes [36]. The Nyquist plot of impedance spectra included a semicircle portion and a linear portion, and the diameter of the semicircular portion at higher frequencies was

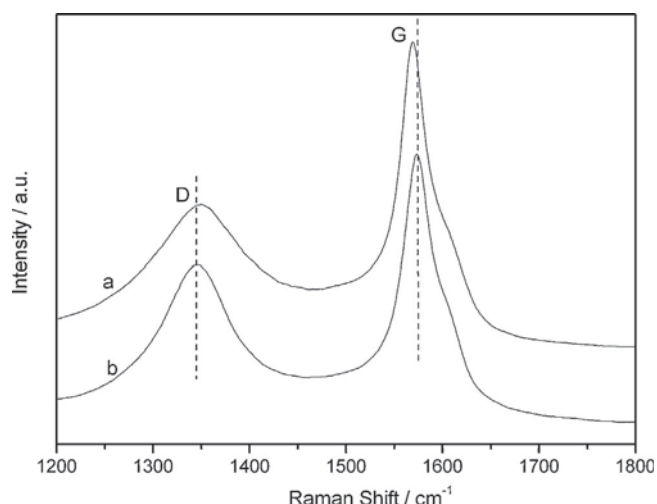


Fig. 2. Raman spectrum of the pRGO in comparison with graphene.

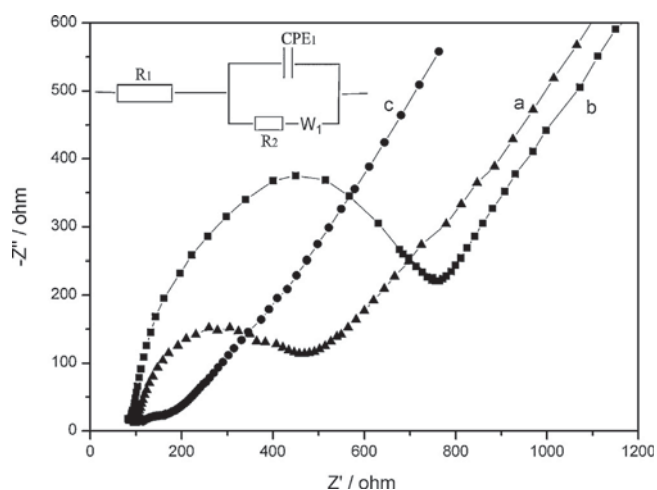


Fig. 3. EIS of (a) bare GCE, (b) CHIT/GCE and (c) pRGO-CHIT/GCE in 0.1 M KCl containing 5.0 mM $K_3[Fe(CN)_6]/K_4[Fe(CN)_6]$. Inset: Equivalent circuit.

equal to the electron transfer resistance R_2 which controlled the electron transfer kinetics of the redox probe at the electrode interface [37–39]. Fig. 3 exhibited the EIS of different electrodes in 0.1 M KCl with equimolar $Fe(CN)_6^{3-/4-}$ ions. The impedance spectrum corresponding to each step was fitted in computer using Zview obtained equivalent circuit (inset in Fig. 3) includes the ohmic resistance of the electrolyte (R_1), the constant phase element (CPE), the Warburg impedance (W_1) and the charge transfer resistance (R_2). As can be seen in the fitting values reported in Table 1, the R_2 at the pRGO-CHIT/GCE (Fig. 3c, $2.72 \Omega cm^2$) was much smaller than that at bare GCE (Fig. 3a, $20.76 \Omega cm^2$) and CHIT/GCE (Fig. 3b, $42.33 \Omega cm^2$), revealing that the pRGO could act as a good electron-transfer interface between the electrochemical probe and the electrode.

Table 1
Fitting values of the equivalent circuit elements.

	bare GCE	CHIT/GCE	pRGO-CHIT/GCE
Capacitance, CPE (F/cm^2)	1.65×10^{-5}	1.54×10^{-4}	7.67×10^{-6}
Resistance, R_1 (Ωcm^2)	7.23	6.32	7.91
Resistance, R_2 (Ωcm^2)	20.76	42.33	2.72
Resistive warburg, W_1-R (Ωcm^2)	372.25	675.98	240.14
Capacitive warburg, W_1-T (Ωcm^2)	1.35	4.83	3.24

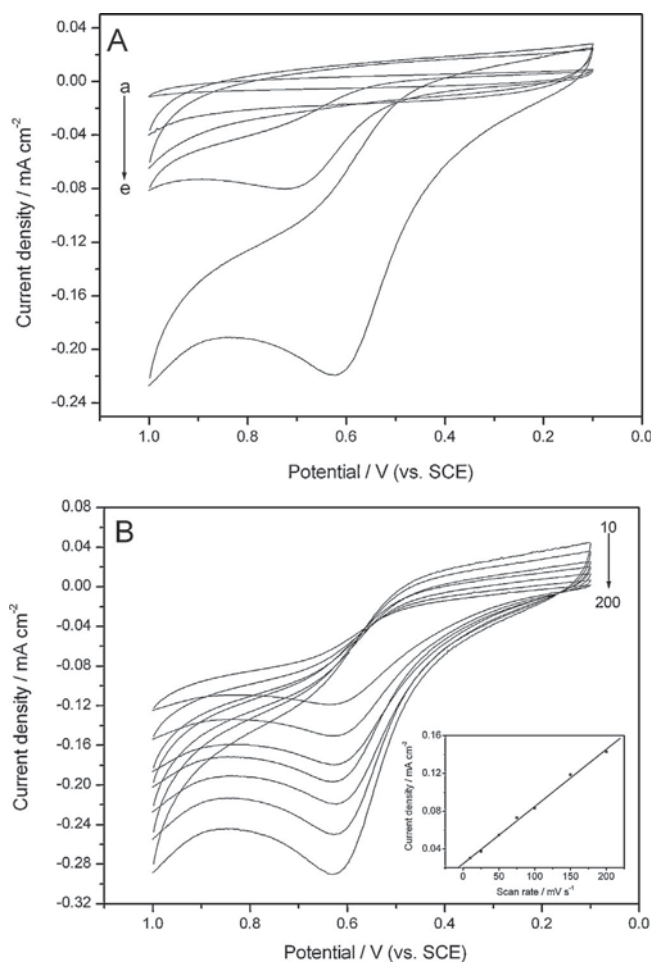


Fig. 4. (A) CV curves of (a) bare GCE, (b) AChE-pRGO-CHIT/GCE in 0.1 M PBS (pH 7.4), (c) pRGO-CHIT/GCE, (d) AChE-CHIT/GCE and (e) AChE-pRGO-CHIT/GCE in 0.1 M PBS (pH 7.4) containing 6.0 mM ATCl. Scan rate: $100 mV s^{-1}$. (B) CV curves of AChE-pRGO-CHIT/GCE in 0.1 M PBS (pH 7.4) containing 6.0 mM ATCl at different scan rates from 10 to $200 mV s^{-1}$. Inset: plots of peak current vs. scan rate.

3.3. Electrochemical behavior of AChE-pRGO-CHIT/GCE

The performance of the fabricated biosensor during stepwise modification was determined by CV method firstly. Fig. 4A presented the CV curves of different electrodes in the absence and presence of ATCl. No peak was observed at different electrodes in 0.1 M PBS without ATCl while an irreversible oxidation peak at 620 mV was observed at AChE-pRGO-CHIT/GCE (curve e) after 6.0 mM ATCl was added, which was corresponding to the oxidation of thiocholine, hydrolysis product of ATCl catalyzed by immobilized AChE [40,41]. Furthermore, the peak current of AChE to ATCl on the pRGO-CHIT/GCE was much higher than that on CHIT/GCE and the peak potential shifted negatively 100 mV, which was attributed to the presence of pRGO providing a conductive pathway for electron-transfer [42,43] and decreasing the over-potential of thiocholine oxidation. The decrease of the over-potential is beneficial for avoiding interference from other electro-active species in biological matrix. Therefore, the pRGO-CHIT/GCE electrode was utilized for OPs detection in our bio-sensing experiments.

Moreover, the effect of scan rate on the CV response of immobilized AChE was also investigated. As displayed in Fig. 4B, the peak current increased while the peak potential shifted slightly with the increase of the scan rate. The peak current exhibited a linear dependence on the scan rates ranging from 10 to $200 mV s^{-1}$ (inset

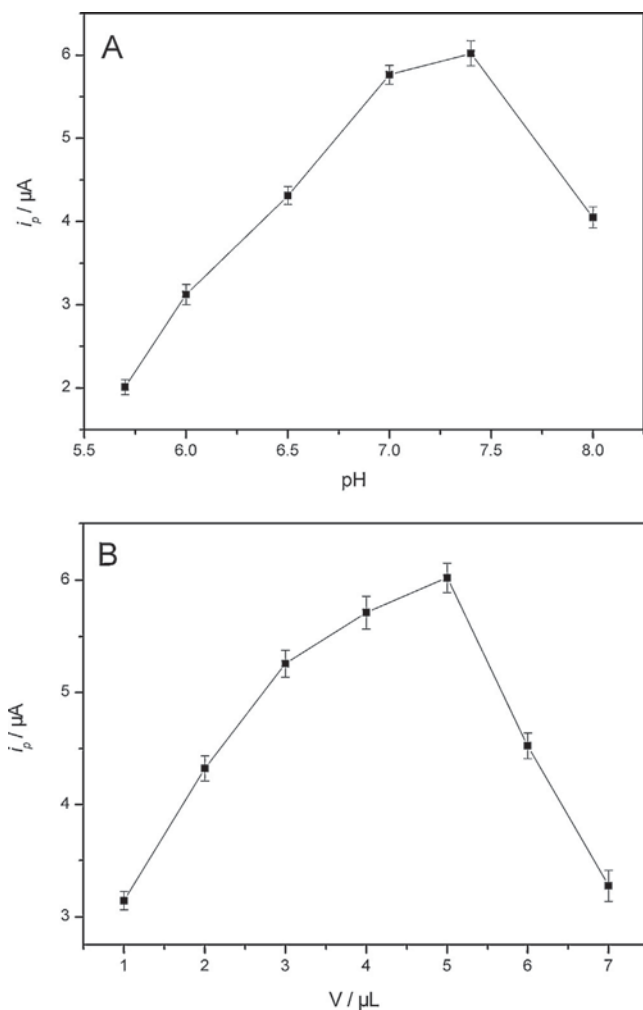


Fig. 5. Effect of the pH (A) and the volume of immobilized AChE (B) on the amperometric response.

in Fig. 4B), indicating a typical surface-controlled electrode process [41].

3.4. Optimization parameters of the biosensor performance

The bioactivity of the immobilized AChE depended on the solution pH. Fig. 5A showed the relationship between catalytic peak current of the response of AChE to ATCl and solution pH. Obviously, the maximum peak current was obtained at about pH 7.4 in the pH range from 5.7 to 8.0. This result was close to that previous report of free AChE, indicating that pRGO sheets did not alter the optimal pH for catalytic behavior of AChE and that the microenvironment surrounded by the immobilized enzyme was easily accessed by the substrate [44]. Thus, pH 7.4 was used in the detection solution.

Another important aspect for the preparation of biosensor was the amount of AChE. The effect of the loading mass on the biosensor ranging from 1 μL to 7 μL was investigated in 0.1 M PBS (pH 7.4) containing 6.0 mM ATCl. As shown in Fig. 5B, the current response increased with increasing amount of AChE and reached the maximum at about 5 μL , then decreased obviously when the amount of AChE was increased further. The phenomenon could be attributed to the higher resistance for the electrochemical processes which was caused by the increase of AChE film's thickness. Therefore, 5 μL AChE was chosen as the optimal enzyme amount.

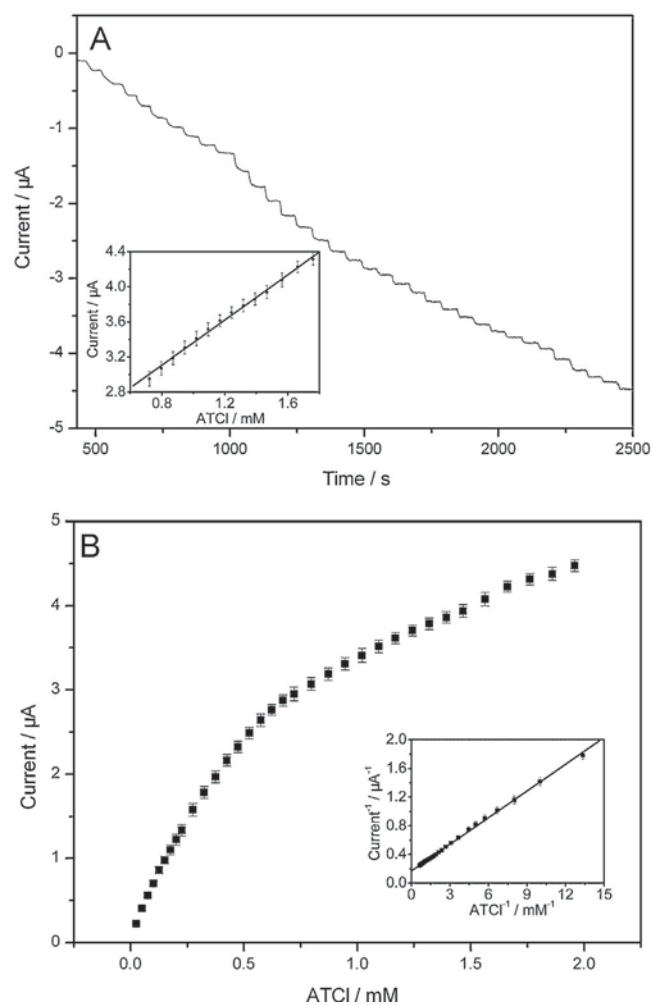


Fig. 6. (A) The i - t curve at the AChE-pRGO-CHIT/GCE for successive addition of ATCl with stirring at the applied potential of 750 mV. Inset: the calibration plot for ATCl determination. (B) The calibration plot for the ATCl sensor. Inset: the Lineweaver-Burk plot of $1/I_{ss}$ vs. $1/C$.

3.5. Calibration plot of ATCl

The typical current-time response curve of the biosensor was obtained by successive additions of the substrate into a stirred cell. As displayed in Fig. 6A, with the increasing concentration of ATCl, the amperometric response increased linearly in the range of 0.72–1.76 mM with a correlation coefficient of 0.998 and then tended to a plateau value, showing a typical Michaelis–Menten process (Fig. 6B). The apparent K_m was calculated to be 0.73 mM according to the Lineweaver–Burk equation. This value was much lower than that of AChE adsorbed on a polyethyleneimine-modified electrode (1.5 mM) [45] and a carbon nanotubes modified electrode (1.75 mM) [46], indicating that the immobilized AChE possessed a higher enzymatic activity and affinity for ATCl due to the excellent electron transfer channels of pRGO.

3.6. Effect of incubation time on inhibition

The inhibition time was one of the most influential parameters in the pesticide analysis. Therefore, the dependence of the carbaryl inhibition on incubation time was also studied. As shown in Fig. 7, carbaryl displayed an increasing inhibition to AChE with the increase of immersion time, and when the incubation time was longer than 12 min, the curve trended to a stable value, indicating that the binding interaction with active target groups in the enzyme

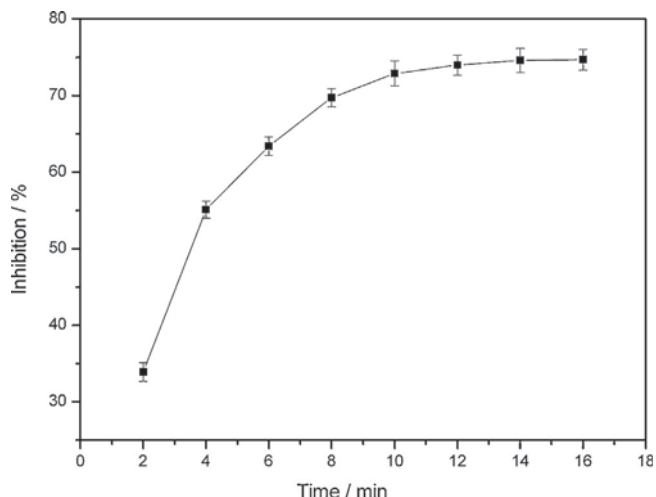


Fig. 7. Effect of incubation time on the response of ATCl after the AChE-pRGO-CHIT/GCE was incubated with $0.3 \mu\text{g mL}^{-1}$ carbaryl solution.

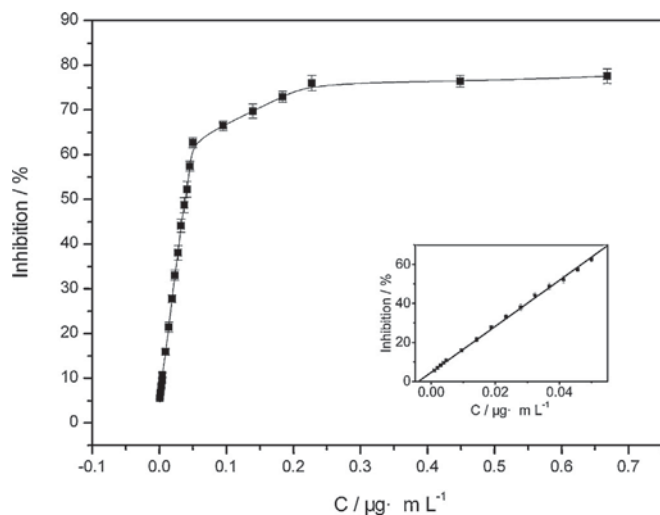


Fig. 8. The Relationship between peak currents and concentrations of carbaryl. Inset: calibration plots for carbaryl determination.

reached saturation. However, the maximum value of inhibition was not 100%, which was likely attributed to the binding equilibrium between pesticides and binding sites in the enzyme [47]. Thus, a 12 min incubation time was used in subsequent experiments.

3.7. Detection of carbaryl

Based on the inhibition of OPs on the immobilized AChE activity, a simple and effective way for monitoring OPs was proposed. As shown in Fig. 8, the inhibition of carbaryl was proportional to its concentration from 0.001 to $0.05 \mu\text{g mL}^{-1}$ with the sensitivity of $1181.20 \text{ ng}^{-1} \text{ mL}$ and the regression coefficients of 0.999. The detection limit is 0.5 ng mL^{-1} ($3 \times$ standard deviation of the blank signal/sensitivity), which was comparable with those reported electrochemical sensors [18,19].

3.8. Reactivation of the biosensor

It was also observed that the as-prepared biosensor inhibited by carbaryl within a certain concentration can resume 91.5% of its original value after immersion in 0.1 M PBS (pH 7.4) for 20 min, indicating that PBS played an important role as a reagent for AChE reactivation. Compared with the previously reported nucleophilic

Table 2

The intra-assay precision of the biosensors.

electrode	1	2	3	4	5
inhibition (%)	49.32	54.02	50.46	52.27	56.89
RSD(%)	5.7				

Table 3

The inter-assay precision of the biosensors.

electrode	1	2	3	4	5
inhibition (%)	57.22	58.50	52.25	47.85	50.69
RSD(%)	8.4				

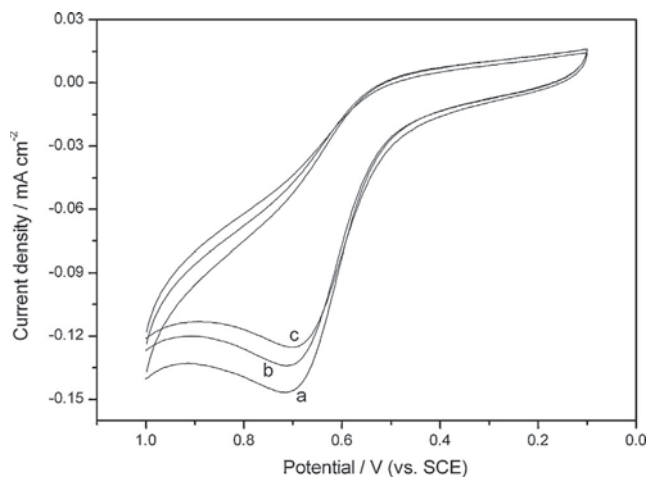


Fig. 9. CV curves of the AChE-pRGO-CHIT/GCE stored at 4°C for (a) 0, (b) 7, (c) 20 days in 0.1 M PBS (pH 7.4) containing 6.0 mM ATCl.

compounds such as pralidoxime iodide as a reagent of reactivation [48], this method was simple and reliable.

3.9. Precision of measurements and stability of biosensor

The intra-assay precision of the biosensors was evaluated by assaying one enzyme electrode for five replicated determinations in 6.0 mM ATCl after being immersed in $0.04 \mu\text{g mL}^{-1}$ of carbaryl for 12 min (Table 2). Similarly, the inter-assay precision or fabrication reproducibility was estimated at five different electrodes (Table 3). The RSD of intra-assay and inter-assay were found to be 5.7% and 8.4%, respectively, indicating good reproducibility.

The long-term storage stability was a critical issue for practical application of the proposed biosensor. Fig. 9 presented the CV curves of the AChE-pRGO-CHIT/GCE stored at 4°C for different time in the presence of ATCl. No obvious decrease in the response of ATCl was observed in the first 7-day storage (curve b). After a 20-day storage period (curve c), the sensor retained 83% of its initial current response (curve a), indicating good stability of biosensor.

4. Conclusions

We have demonstrated a simple and efficient strategy for immobilizing AChE and developed a sensitive sensor for detection of carbaryl pesticide by integrating pRGO nano-sheets. Due to the excellent electron-transfer channels of the support, the immobilized AChE possesses higher enzymatic activity and affinity to ATCl. Based on the change in electrochemical response of enzymatic activity induced by OPs pesticide, an electrochemical technique with good reproducibility, stability and fast response for OPs pesticide is successfully developed. With the development of pRGO in the application of carbaryl detection, we expect that the functional

prGO will find important and widespread applications in other OPs pesticide exposure.

Acknowledgements

The authors thank the National Natural Science Foundation of China (21073115, 20604014), Natural Science Foundation (2012021021-3) of Shanxi province, the Program for New Century Excellent Talents in University (NCET-10-0926) of China and the returned personnel of scientific research project of Shanxi (2011-003).

References

- [1] X. Sun, X.Y. Wang, Acetylcholinesterase biosensor based on Prussian blue-modified electrode for detecting organophosphorous pesticides, *Biosensors and Bioelectronics* 25 (2010) 2611–2614.
- [2] J.M. Gong, L.Y. Wang, L.Z. Zhang, Electrochemical biosensing of methyl parathion pesticide based on acetylcholinesterase immobilized onto Au-polypyrrole interlaced network-like nanocomposite, *Biosensors and Bioelectronics* 24 (2009) 2285–2288.
- [3] A. Mulchandani, P. Mulchandani, I. Kaneva, W. Chen, Biosensor for direct determination of organophosphate nerve agents using recombinant *Escherichia coli* with surface-expressed organophosphorus hydrolase. 1. potentiometric microbial electrode, *Analytical Chemistry* 70 (1998) 4140–4145.
- [4] G.D. Liu, Y.H. Lin, Biosensor based on self-assembling acetylcholinesterase on carbon nanotubes for flow injection/amperometric detection of organophosphate pesticides and nerve agents, *Analytical Chemistry* 78 (2006) 835–843.
- [5] D. Du, J.W. Ding, J. Cai, A.D. Zhang, One-step electrochemically deposited interface of chitosan-gold nanoparticles for acetylcholinesterase biosensor design, *Journal of Electroanalytical Chemistry* 605 (2007) 53–60.
- [6] J.M. Gong, T. Liu, D.D. Song, X.B. Zhang, L.Z. Zhang, One-step fabrication of three-dimensional porous calcium carbonate-chitosan composite film as the immobilization matrix of acetylcholinesterase and its biosensing on pesticide, *Electrochemistry Communications* 11 (2009) 1873–1876.
- [7] D. Du, M.H. Wang, J. Cai, A.D. Zhang, Sensitive acetylcholinesterase biosensor based on assembly of β -cyclodextrins onto multiwall carbon nanotubes for detection of organophosphates pesticide, *Sensors and Actuators B* 146 (2010) 337–341.
- [8] D. Du, W.J. Chen, J. Cai, J. Zhang, F.G. Qu, H.B. Li, Development of acetylcholinesterase biosensor based on CdTe quantum dots modified cysteamine self-assembled monolayers, *Journal of Electroanalytical Chemistry* 623 (2008) 81–85.
- [9] R. Sinha, M. Ganesana, S. Andreescu, L. Stanciu, AChE biosensor based on zinc oxide sol-gel for the detection of pesticides, *Analytica Chimica Acta* 661 (2010) 195–199.
- [10] S. Alwarappan, A. Erdem, C. Liu, C.Z. Li, Probing the electrochemical properties of graphene nanosheets for biosensing applications, *Journal of Physical Chemistry C* 13 (2009) 8853–8857.
- [11] S. Alwarappan, C. Liu, A. Kumar, C.Z. Li, Enzyme-doped graphene nanosheets for enhanced glucose biosensing, *Journal of Physical Chemistry C* 114 (2010) 12920–12924.
- [12] S. Alwarappan, S. Boyapalle, A. Kumar, C.Z. Li, S. Mohapatra, Comparative study of single-, few-, and multilayered graphene toward enzyme conjugation and electrochemical response, *Journal of Physical Chemistry C* 116 (2012) 6556–6559.
- [13] S. Alwarappan, R.K. Joshi, M.K. Ram, A. Kumar, Electron transfer mechanism of cytochrome c at graphene electrode, *Applied Physics Letters* 96 (2010) 263702.
- [14] S. Alwarappan, K. Cissell, S. Dixit, C.Z. Li, S. Mohapatra, Chitosan-modified graphene electrodes for DNA mutation analysis, *Journal of Electroanalytical Chemistry* 686 (2012) 69–72.
- [15] S. Stankovich, D.A. Dikin, G.H.B. Dommett, K.M. Kohlhaas, E.J. Zimney, E.A. Stach, R.D. Piner, S.T. Nguyen, R.S. Ruoff, Graphene-based composite materials, *Nature* 442 (2006) 282–286.
- [16] Z.M. Ao, J. Yang, S. Li, Q. Jiang, Enhancement of CO detection in Al doped graphene, *Chemical Physics Letters* 461 (2008) 276–279.
- [17] Y.P. Li, G.Y. Han, Ionic liquid-functionalized graphene for fabricating an amperometric acetylcholinesterase biosensor, *Analyst* 137 (2012) 3160–3165.
- [18] K. Wang, Q. Liu, L. Dai, J. Yan, C. Ju, B. Qiu, X. Wu, A highly sensitive and rapid organophosphate biosensor based on enhancement of CdS-decorated graphene nanocomposite, *Analytica Chimica Acta* 695 (2011) 84–88.
- [19] K. Wang, H.N. Li, J. Wu, C. Ju, J.J. Yan, Q. Liu, B. Qiu, TiO₂-decorated graphene nanohybrids for fabricating an amperometric acetylcholinesterase biosensor, *Analyst* 136 (2011) 3349–3354.
- [20] Y. Wang, S. Zhang, D. Du, Y. Shao, Z. Li, J. Wang, M.H. Engelhard, J. Li, Y. Lin, Self assembly of acetylcholinesterase on a gold nanoparticles-graphene nanosheet hybrid for organophosphate pesticide detection using polyelectrolyte as a linker, *Journal of Materials Chemistry* 21 (2011) 5319–5325.
- [21] T. Liu, H. Su, X. Qu, P. Ju, L. Cui, S. Ai, Acetylcholinesterase biosensor based on 3-carboxyphenylboronic acid/reduced graphene oxide-gold nanocomposites modified electrode for amperometric detection of organophosphorus and carbamate pesticides, *Sensors and Actuators B* 160 (2011) 12551261.
- [22] D.E. Jiang, V.R. Cooper, S. Dai, Porous graphene as the ultimate membrane for gas separation, *Nano Letters* 9 (2009) 4019–4024.
- [23] A. Du, Z. Zhu, S.C. Smith, Multifunctional porous graphene for nanoelectronics and hydrogen storage: new properties revealed by first principle calculations, *Journal of the American Chemical Society* 132 (2010) 2876–2877.
- [24] J. Bai, X. Zhong, S. Jiang, Y. Huang, X. Duan, Graphene nanomesh, *Nature Nanotechnology* 5 (2010) 190–194.
- [25] Y. Zhu, S. Murali, M.D. Stoller, K.J. Ganesh, W. Cai, P.J. Ferreira, A. Pirkle, R.M. Wallace, K.A. Cychosz, M. Thommes, D. Su, E.A. Stach, R.S. Ruoff, Carbon-based supercapacitors produced by activation of graphene, *Science* 332 (2011) 1537–1541.
- [26] T.H. Han, Y.K. Huang, A.T.L. Tan, V.P. Dravid, J. Huang, Steam etched porous graphene oxide network for chemical sensing, *Journal of the American Chemical Society* 133 (2011) 15264–15267.
- [27] M.A. Harmer, W.E. Farneth, Q. Sun, High surface area nafion resin/silica nanocomposites: a new class of solid acid catalyst, *Journal of the American Chemical Society* 118 (1996) 7708–7715.
- [28] J. Sarkar, V.T. John, J. He, C. Brooks, D. Gandhi, A. Nunes, G. Ramanath, A. Bose, Surfactant-Templated synthesis and catalytic properties of patterned nanoporous titania supports loaded with platinum nanoparticles, *Chemistry of Materials* 20 (2008) 5301–5306.
- [29] T. Hasell, C.D. Wood, R. Clowes, J.T.A. Jones, Y.Z. Khimyak, D.J. Adams, A.I. Cooper, Palladium nanoparticle incorporation in conjugated microporous polymers by supercritical fluid processing, *Chemistry of Materials* 22 (2010) 557–564.
- [30] S. Kim, Y. Kim, Y. Ko, J. Cho, Electrochemical Sensors based on porous nanocomposite films with weak polyelectrolyte-stabilized gold nanoparticles, *Journal of Materials Chemistry* 21 (2011) 8008–8013.
- [31] L.L. Zhang, X. Zhao, M.D. Stoller, Y. Zhu, H. Ji, S. Murali, Y. Wu, S. Perales, B. Cleveenger, R.S. Ruoff, Highly conductive and porous activated reduced graphene oxide films for high-power supercapacitors, *Nano letters* 12 (2012) 1806–1812.
- [32] M.G. Zhang, A. Smith, W. Gorski, Carbon nanotube-chitosan system for electrochemical sensing based on dehydrogenase enzymes, *Analytical Chemistry* 76 (2004) 5045–5050.
- [33] A.C. Ferrari, J.C. Meyer, V. Scardaci, C. Casiraghi, M. Lazzeri, F. Mauri, S. Piscanec, D. Jiang, K.S. Novoselov, S. Roth, A.K. Geim, Raman spectrum of graphene and graphene layers, *Physical Review Letters* 97 (2006) 187401–187404.
- [34] D.V. Kosynkin, A.L. Higginbotham, A. Sinitskii, J.R. Lomeda, A. Dimiev, B.K. Price, J.M. Tour, Longitudinal unzipping of carbon nanotubes to form graphene nanoribbons, *Nature* 458 (2009), 872–U5.
- [35] H.L. Guo, X.F. Wang, Q.Y. Qian, F.B. Wang, X.H. Xia, *ACS Nano* 3 (2009) 2653–2659.
- [36] Y. Liu, R. Yuan, Y.Q. Chai, D.P. Tang, J.Y. Dai, X. Zhong, Direct electrochemistry of horseradish peroxidase immobilized on gold colloid/cysteine/nafiion-modified platinum disk electrode, *Sensors and Actuators B* 115 (2006) 109–115.
- [37] X.H. Kang, J. Wang, H. Wu, I.A. Aksay, J. Liu, Y.H. Lin, Glucose Oxidase-graphene-chitosan modified electrode for direct electrochemistry and glucose sensing, *Biosensors and Bioelectronics* 25 (2009) 901–905.
- [38] I. Hafaeidh, H. Baccar, T. Ktari, A. Abdelghani, Electrochemical characterization of streptavidin-HRP immobilized on multiwall carbon nanotubes for biosensor applications, *Journal of Biomaterial and Nanobiotechnology* 3 (2012) 31–36.
- [39] C. Essegheier, Y. Bergaoui, H. ben Fredj, A. Tlili, S. Helali, S. Ameer, A. Abdelghani, Impedance Spectroscopy on Immobilized Streptavidin Horseradish Peroxidase Layer for Biosensing, *Sensors and Actuators B: Chemical* 134 (2008) 112–116.
- [40] D. Du, M.H. Wang, J. Cai, Y.H. Qin, A.D. Zhang, One-step synthesis of multiwalled carbon nanotubes-gold nanocomposites for fabricating amperometric acetylcholinesterase biosensor, *Sensors and Actuators B* 143 (2010) 524–529.
- [41] D. Du, J.W. Ding, J. Cai, A.D. Zhang, Determination of carbaryl pesticide using amperometric acetylcholinesterase sensor formed by electrochemically deposited chitosan, *Colloids and Surfaces B: Biointerfaces* 58 (2007) 145–150.
- [42] K. Wang, Q. Liu, Q.M. Guan, J. Wu, H.N. Li, J.J. Yan, Enhanced direct electrochemistry of glucose oxidase and biosensing for glucose via synergy effect of graphene and CdS nanocrystals, *Biosensors and Bioelectronics* 26 (2011) 2252–2257.
- [43] D. Du, S.Z. Chen, J. Cai, A.D. Zhang, Immobilization of acetylcholinesterase on gold nanoparticles embedded in sol-gel film for amperometric detection of organophosphorous insecticide, *Biosensors and Bioelectronics* 23 (2007) 130–134.
- [44] M. Bernabei, S. Chiavari, C. Cremisini, G. Palleschi, Anticholinesterase activity measurement by a choline biosensor: application in water analysis, *Biosensors and Bioelectronics* 8 (1993) 265–271.
- [45] A. Vakurov, C.E. Simpson, C.L. Daly, T.D. Gibson, P.A. Millner, Acetylcholinesterase-based biosensor electrodes for organophosphate pesticide detection I. Modification of carbon surface for immobilization of acetylcholinesterase, *Biosensors and Bioelectronics* 20 (2004) 1118–1125.
- [46] G.D. Liu, Y.H. Lin, Biosensor based on self-assembling acetylcholinesterase on carbon nanotubes for flow injection/amperometric detection of organophosphate pesticides and nerve agents, *Analytical Chemistry* 78 (2006) 835–843.
- [47] J. Chen, D. Du, F. Yan, H.X. Ju, H.Z. Lian, Electrochemical antitumor drug sensitivity test for leukemia K562 cells at a carbon-nanotube-modified electrode, *Chemistry – A European Journal* 11 (2005) 1467–1472.
- [48] D. Du, X. Huang, J. Cai, A.D. Zhang, Amperometric detection of triazophos pesticide using acetylcholinesterase biosensor based on multiwall carbon nanotube-chitosan matrix, *Sensors and Actuators B* 127 (2007) 531–535.

Biographies

Yanping Li earned her PhD in inorganic chemistry from Shanxi University in 2007. Now, she is an associate professor in Shanxi University. Her research interests include the synthesis and functionalization of carbon nanomaterials for their applications in biosensing.

Yunfei Bai is a master student in inorganic chemistry in Shanxi University. His research interests include the synthesis and functionalization of carbon nanomaterials for their applications in biosensing.

Gaoyi Han earned his PhD in inorganic chemistry from Nanjing University in 2001. Now, he is a professor in Shanxi University. His research interests include the synthesis and performance of the nanomaterials of carbon and conducting polymers.

Miaoyu Li earned her PhD in inorganic chemistry from Shanxi University in 2011. Now, she is a lecturer in Shanxi University. Her research interests include the synthesis and performance of carbon nanomaterials.